Applied Physics Letters

25 Gbit/s differential phase-shift-keying signal generation using directly modulated quantum-dot semiconductor optical amplifiers

Cite as: Appl. Phys. Lett. **106**, 213501 (2015); https://doi.org/10.1063/1.4921785
Submitted: 10 April 2015 . Accepted: 16 May 2015 . Published Online: 26 May 2015

A. Zeghuzi, H. Schmeckebier, M. Stubenrauch, C. Meuer, C. Schubert, C.-A. Bunge, and D. Bimberg

AIP Publishing

25 Gbit/s differential phase-shift-keying signal generation using directly modulated quantum-dot semiconductor optical amplifiers

A. Zeghuzi,[1,a)] H. Schmeckebier,[1] M. Stubenrauch,[1] C. Meuer,[2] C. Schubert,[2] C.-A. Bunge,[3] and D. Bimberg[1,b)]
[1]*Department of Solid-State Physics, Technische Universitaet Berlin, Hardenbergstr. 36, 10623 Berlin, Germany*
[2]*Fraunhofer Institute for Telecommunications, Heinrich Hertz Institute, Einsteinufer 37, 10587 Berlin, Germany*
[3]*Hochschule fuer Telekommunikation Leipzig (HfTL), Gustav-Freytag-Str. 43-45, 04277 Leipzig, Germany*

(Received 10 April 2015; accepted 16 May 2015; published online 26 May 2015)

Error-free generation of 25-Gbit/s differential phase-shift keying (DPSK) signals via direct modulation of InAs quantum-dot (QD) based semiconductor optical amplifiers (SOAs) is experimentally demonstrated with an input power level of −5 dBm. The QD SOAs emit in the 1.3-μm wavelength range and provide a small-signal fiber-to-fiber gain of 8 dB. Furthermore, error-free DPSK modulation is achieved for constant optical input power levels from 3 dBm down to only −11 dBm for a bit rate of 20 Gbit/s. Direct phase modulation of QD SOAs via current changes is thus demonstrated to be much faster than direct gain modulation. © *2015 AIP Publishing LLC*.
[http://dx.doi.org/10.1063/1.4921785]

In the last decades, numerous groups have investigated quantum-dot (QD) based devices for fiber-optic communication in the 1.31-μm and 1.55-μm wavelength ranges, as they offer distinct advantages in comparison to standard gain media like quantum well or bulk.[1] Important advantages are a broad gain bandwidth,[2] high temperature stability,[3,4] low threshold currents,[5] ultra-fast dynamics within the QDs,[6–8] and high saturation output power.[9]

Using directly modulated devices reduces the number of components and thus costs in optical networks. Directly modulated QD lasers were used to generate on–off keying (OOK) signals with bit rates up to 25 Gbit/s.[9,10] The drive current as well as the modulation voltage for optimum operation depends on the system application. The small-signal modulation bandwidth in QD devices is low at currents close to the threshold current and usually peaks at ten to twenty times the threshold current, which is often close to the saturation optical output power.[10] The optimum eye opening in terms of modulation depth and extinction ratio however is usually observed to be at a much lower current between these two extreme points. The limiting factors for small signal modulation of QD lasers are the QD ground-state (GS) gain saturation.[10] Gain saturation induced output power limitation of QD devices presents an advantage for the generation of phase coded signals in direct modulation schemes. In contrast to OOK signals, phase coded signals such as differential phase shift keying (DPSK) offer a 3-dB reduction in required optical-signal-to-noise ratio and are more robust to, e.g., fiber nonlinearity induced effects.[11,12]

Most QD devices are based on the GS excitonic transition. The QD excited states (ES) and in particular, the higher energy levels of the surrounding quantum wells (QWs) and/or bulk material are thought to act solely as the carrier reservoir.[13] In contrast to QW and bulk based devices, in QD devices the real and imaginary parts of the susceptibility are decoupled if the emitting state is saturated.[14] The gain is defined by the QDs, whereas the QD surrounding material within the waveguide controls the phase probed by the optical wave. Thus, a saturated QD laser enables phase changes independent of amplitude changes. Semiconductor lasers in general show thermal rollover effects. This potentially limits the drive voltage for direct phase modulation. The absolute phase change reached without amplitude variation is therefore limited. Using saturated QD semiconductor optical amplifiers (SOAs) for direct phase modulation instead overcomes this limitation, because an increase of the drive current only slightly decreases the gain, and thus larger drive voltages are supported. In addition, in SOAs most signal parameters, such as wavelength and optical output power, can be chosen independently of each other. As a potential application, directly modulated SOAs can be used as reflective SOAs (R-SOAs) for color-free operation in passive optical networks.[15,16]

The concept of directly OOK modulated SOAs has been demonstrated for different material systems up to 10 Gbit/s,[15,17,18] whereas direct DPSK modulation of DFB lasers is presented up to 16 Gbit/s.[19] In this paper, we present directly modulated error-free DPSK generation at bit rates up to 25 Gbit/s using SOAs.

The experimental setup is schematically shown in Fig. 1. In the transmitter, the well-controlled optical output of an external cavity laser (ECL) is injected into the QD SOA with its polarization aligned to the TE axis. The QD SOA is driven at constant bias. An electrical non-return-to-zero signal with a pseudo-random binary sequence (PBRS) of a length of 27-1 bits, generated by a 56 Gbit/s bit-pattern generator (BPG) is superimposed. The modulated optical output of the QD SOA passes an optical 2-nm band-pass filter to suppress the ASE.

The active region of the 2-mm-long QD SOA is composed of 10 layers of self-organized In(Ga)As QDs, each

a)Author to whom correspondence should be addressed. Electronic mail: zeghuzi@mailbox.tu-berlin.de
b)Also with King Abdulaziz University, 22254 Jeddah, Saudi Arabia.

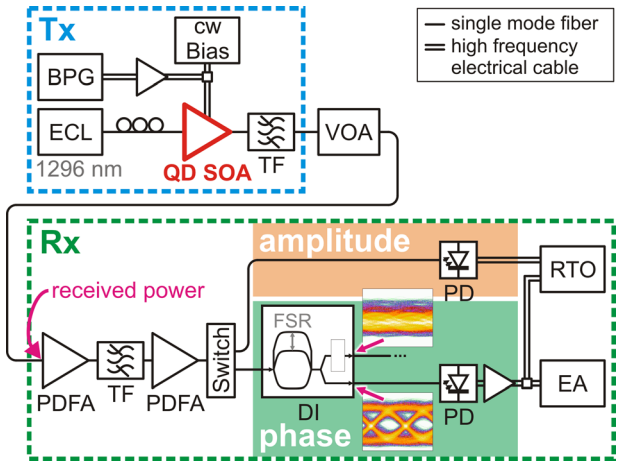

FIG. 1. Experimental setup with transmitter (Tx) and receiver (Rx). The plotted eye patterns show exemplarily the output signals at the DI for a bit-rate of 20 Gbit/s and QD SOA input power of −5 dBm. BPG: bit pattern generator, DI: delay interferometer, EA: error analyzer, ECL: external cavity laser, FSR: free-spectral range, PD: photo diode, PDFA: praseodymium-doped fiber amplifier, QD SOA: quantum-dot semiconductor optical amplifier, RTO: real-time oscilloscope, TF: tunable filter, VOA: variable optical attenuator.

capped with an InGaAs QW (dots-in-a-well (DWELL) structure) and separated by a 33-nm-wide GaAs spacer layer.[20] The active region is embedded between $Al_{0.15}Ga_{0.85}As$ upper and bottom cladding layers. The 4-μm-wide deeply etched ridge waveguide is tilted by an angle of 6.8° with respect to the facet normal to suppress the onset of lasing. The facets are additionally anti-reflection coated. The structure is planarized with Benzocyclobutene (BCB) and both contacts are led to the top. The device is contacted with a RF probe head.

The optical input power into the receiver can be controlled with a variable optical attenuator (VOA). The receiver consists of an optical preamplifier stage, based on two praseodymium-doped fiber amplifiers (PDFAs) with a 2-nm FWHM tunable filter in between to suppress the ASE of the first amplifier. The second amplifier is set to a constant optical output power mode. The optical signal is led to different receiver parts via an optical switch, depending on the modulation type. The amplitude-modulated signal is directly detected using a 50 GHz photodiode (PD). For phase coded signals, a delay interferometer (DI) is used to demodulate the signal.[21] In the DI, one beam is time delayed by one bit duration with respect to the other. The two beams interfere at the output, where amplitude and phase are processed, and the phase modulation is transformed to amplitude modulation. The DI output was measured single ended with a 50 GHz photodiode (PD) and analyzed with respect to signal quality via eye-pattern measurements using an 80-GSa/s real-time oscilloscope and bit-error-ratio (BER) measurements by means of a 56-Gbit/s error analyzer.

The amplified spontaneous emission (ASE) spectra as well as fiber-to-fiber gain and noise figure of the QD SOA are shown in Fig. 2. The GS ASE is centered around 1300 nm, saturates at a current of around 100 mA, and stays constant in power up to a current of around 200 mA. The peak wavelength shifts with increasing current by 7 nm due to device heating. At an ECL wavelength of 1296 nm and currents varying from 100 mA to 200 mA, the power

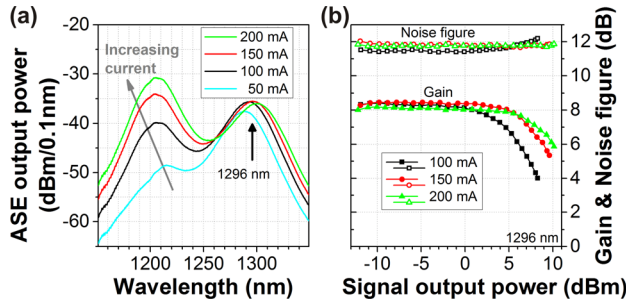

FIG. 2. (a) QD SOA single-facet fiber-coupled ASE spectrum for different drive currents. (b) Fiber-to-fiber gain as well as fiber-to-fiber noise figure for different drive currents and a wavelength of 1296 nm.

variation ΔP is only 0.6 dBm. Under modulation within this current range, the variation should be still smaller, because heating effects will not result in a decrease of the ASE power anymore. In this current range, the linear fiber-to-fiber gain is larger than 8 dB, corresponding to a chip gain of 17 dB, taking into account 4.5 dB coupling losses per facet. The saturation output power in fiber is 7.0 dBm, 9.6 dBm, and 11.0 dBm for currents of 100 mA, 150 mA, and 200 mA, respectively. The fiber-to-fiber noise figure is between 11.4 and 12.2 dB.

At large injection currents, the carrier reservoir remains highly populated during photon-induced depletion of the QD GS and thus the GS recovers on a sub-picosecond scale.[22] Direct modulation of SOAs induces a change of the current density, resulting in a refractive index change. For a saturated QD SOA, the carrier density change of the reservoir has a negligible influence on the GS gain for moderate modulation amplitude levels. The refractive-index change within the waveguide leads to a phase change of the amplified optical wave. Consequently, at a constant drive current between 100 mA and 200 mA amplitude modulation is suppressed, enabling phase without amplitude modulation.

An input wavelength of 1296 nm was chosen, offering the highest available gain. The constant current as well as the modulation swing was adjusted by optimizing the eye pattern as well as the BER. For the lowest available modulation speed of 6 Gbit/s an on–off keying disturbed eye structure was observed if the current is reduced below 100 mA. However, at a current above 100 mA no visible on–off keying eye structure is detected.

The optimal modulation point has to be adjusted as a trade-off between two effects. A lower electrical modulation amplitude reduces the refractive-index change and thus the phase shift, whereas a higher electrical modulation amplitude will increase it. However, signal distortions due to gain modulations might increase for larger modulation amplitudes.

For the direct phase modulation, a current of 125 mA and a peak-to-peak voltage of 3 V were identified as the optimum point of operation. Only one of the two DI output ports showed an open eye pattern, whereas the other port showed only a distorted eye pattern (see Fig. 1). Changing the DI phase by 180° inverts the two DI output ports. A simple simulation of the DI output ports with DPSK input signals and different distorting amplitude modulation levels indicates that indeed a residual amplitude modulation may lead to such an effect. A phase shift deviating from 180° would only

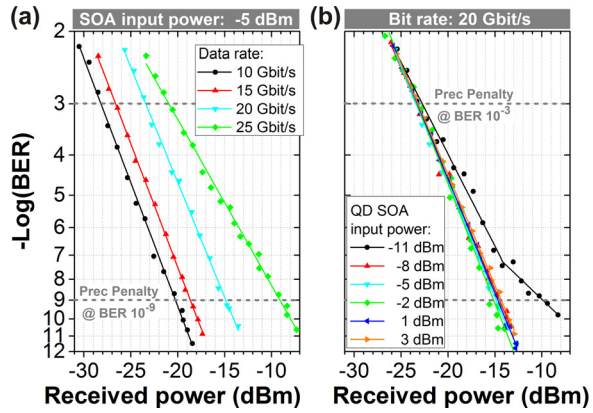

FIG. 3. Measured BER versus received power for (a) varying data rate and for (b) varying QD SOA input power. The power penalties at a BER of 10^{-9} and 10^{-3} are evaluated in Fig. 4.

influence the eye opening but cannot be the reason for the effect.

As a figure of merit of the signal quality, BER measurements were conducted for different modulation speeds for a fixed QD SOA input power level of −5 dBm (Fig. 3(a)), as well as for different QD SOA optical input-power levels and a fixed modulation speed of 20 Gbit/s (Fig. 3(b)). The received power and optical signal-to-noise ratio (OSNR) penalties are evaluated at a BER of 10^{-3} and 10^{-9} (error free) with respect to the best corresponding BER curve marked by "Reference" in Figs. 4(a) and 4(b). As the receiver requires a constant received energy per bit for a comparable BER, the BER-curves are shifted towards larger received powers with increasing bit rate. Up to 20 Gbit/s, the slope of the BER curves remains nearly constant, but at 25 Gbit/s the slope flattens, possibly due to parasitic bandwidth limitation of the QD SOA. However, no error-floor is observed for all measured modulation speeds. The corresponding eye patterns are shown in Fig. 4(c) using the DI based receiver (labeled DPSK) and the direct-detection receiver (labeled OOK), respectively. With increasing modulation speed, the amplitude swing of the OOK eye pattern decreases, indicating a reduced amplitude modulation of the generated signal. Furthermore the level variation of the DPSK eye is reduced with increasing modulation speed, possibly due to reduced amplitude swing.

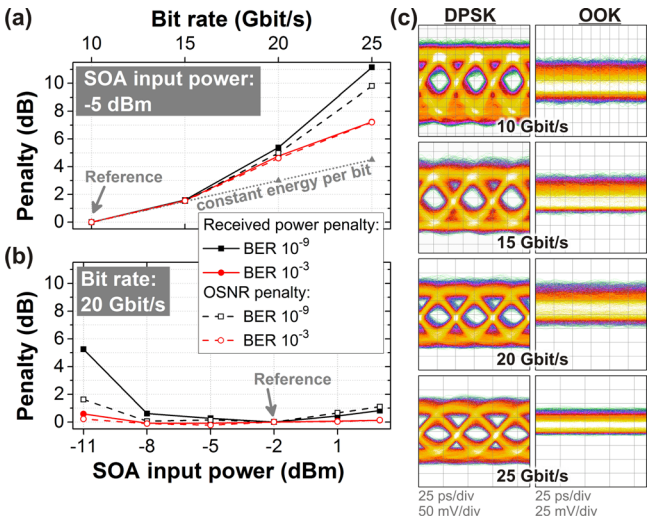

FIG. 4. Received power and OSNR penalty at a BER of 10^{-9} and 10^{-3} for (a) different data rates and (b) SOA input powers with respect to the BER curve marked with "Reference." (c) Eye patterns for different bit rates using the DI-based receiver (DPSK) and the direct detection receiver (OOK), respectively, recorded at a BER of 10^{-9}.

Within an input power range from 3 dBm to −8 dBm, the signal quality in terms of required received power and OSNR is comparable to the "Reference," demonstrated by negligible penalties (Fig. 4(b)). The shape and level variation of the corresponding eye diagrams are comparable to the 20 Gbit/s eye pattern shown in Fig. 4(c) (measured for −5 dBm). Decreasing the input power further to −11 dBm leads to an error floor and finally to power penalties of about 0.6 dB and 5.2 dB for BERs of 10^{-3} and 10^{-9}, respectively. However, even for this input power error-free operation is obtained.

The time constant of the RF-signal transition induced adiabatic chirp in the reservoir is smaller than the effective time constant of the reservoir, which includes all carrier relaxation processes. The differential detection is solely based on those fast contributions to the total phase change within the reservoir.

The strongly reduced coupling between refractive index and gain in QD SOAs driven at high injection currents was used for direct phase modulation. Direct on–off keying modulation of the QD SOA was limited to below 6 Gbit/s. Error–free (BER $< 10^{-9}$) direct DPSK modulation was achieved up to a bit rate of 25 Gbit/s with small or negligible amplitude modulation. Furthermore, error-free DPSK modulation with a bit rate of 20 Gbit/s was achieved for constant optical input power levels from 3 dBm down to only −11 dBm, where the QD SOA shows a small-signal fiber-to-fiber gain of 8 dB. In conclusion, direct phase modulation via a current change is much faster than direct gain modulation, enabling direct DPSK modulation at high bit rates.

This work was supported by Kylia with the Delay interferometer and funded by the collaborative research center CRC 787 of the German Research Foundation (DFG).

[1]D. Bimberg, Electron. Lett. **44**, 390 (2008).
[2]D. Bimberg, M. Grundmann, N. N. Ledentsov, S. S. Ruvimov, P. Werner, U. Richter, J. Heydenreich, V. M. Ustinov, P. S. Kop'ev, and Z. I. Alferov, Thin Solid Films **267**, 32 (1995).
[3]O. B. Shchekin and D. G. Deppe, Appl. Phys. Lett. **80**, 3277 (2002).
[4]S. S. Mikhrin, A. R. Kovsh, I. L. Krestnikov, A. V. Kozhukhov, D. A. Livshits, N. N. Ledentsov, Y. M. Shernyakov, I. I. Novikov, M. V. Maximov, V. M. Ustinov, and Z. I. Alferov, Semicond. Sci. Technol. **20**, 340 (2005).
[5]R. L. Sellin, C. Ribbat, M. Grundmann, N. N. Ledentsov, and D. Bimberg, Appl. Phys. Lett. **78**, 1207 (2001).
[6]T. Vallaitis, C. Koos, R. Bonk, W. Freude, M. Laemmlin, C. Meuer, D. Bimberg, and J. Leuthold, Opt. Express **16**, 170 (2008).
[7]T. W. Berg, S. Bischoff, I. Magnusdottir, and J. Mørk, IEEE Photonics Technol. Lett. **13**, 541 (2001).
[8]I. O'Driscoll, T. Piwonski, J. Houlihan, G. Huyet, R. J. Manning, and B. Corbett, Appl. Phys. Lett. **91**, 263506 (2007).
[9]A. V. Uskov, E. P. O'Reilly, M. Laemmlin, N. N. Ledentsov, and D. Bimberg, Opt. Commun. **248**, 211 (2005).
[10]D. Arsenijević, A. Schliwa, H. Schmeckebier, M. Stubenrauch, M. Spiegelberg, D. Bimberg, V. Mikhelashvili, and G. Eisenstein, Appl. Phys. Lett. **104**, 181101 (2014).

[11]S. Ferber, R. Ludwig, C. Boerner, A. Wietfeld, B. Schmauss, J. Berger, C. Schubert, G. Unterboersch, and H. G. Weber, Electron. Lett. **39**, 1458 (2003).
[12]A. H. Gnauck and P. J. Winzer, IEEE J. Lightwave Technol. **23**, 115 (2005).
[13]C. Meuer, J. Kim, M. Laemmlin, S. Liebich, A. Capua, G. Eisenstein, A. R. Kovsh, S. S. Mikhrin, I. L. Krestnikov, and D. Bimberg, Opt. Express **16**, 8269 (2008).
[14]A. V. Uskov, E. P. O'Reilly, D. McPeake, N. N. Ledentsov, D. Bimberg, and G. Huyet, Appl. Phys. Lett. **84**, 272 (2004).
[15]M. Omella, I. Papagiannakis, B. Schrenk, D. Klonidis, J. A. Lázaro, A. N. Birbas, J. Kikidis, J. Prat, and I. Tomkos, Opt. Express **17**, 5008 (2009).
[16]H. Kim, IEEE Photonics Technol. Lett. **23**, 965 (2011).
[17]B. Schrenk, G. De Valicourt, M. Omella, J. A. Lazaro, R. Brenot, and J. Prat, IEEE Photonics Technol. Lett. **22**, 392 (2010).
[18]D. C. Kim, B.-S. Choi, H.-S. Kim, K. S. Kim, K.-H. Yoon, O.-K. Kwon, and D.-K. Oh, Jpn. J. Appl. Phys., Part 1 **48**, 120209 (2009).
[19]A. S. Karar, Y. Gao, K. P. Zhong, J. H. Ke, and J. C. Cartledge, in *2012 38th European Conference and Exhibition on Optical Communication (ECOC)* (Osa, Washington, D.C., 2012), pp. 1–3.
[20]A. R. Kovsh, N. A. Maleev, A. E. Zhukov, S. S. Mikhrin, A. P. Vasil'ev, E. A. Semenova, Y. M. Shernyakov, M. V. Maximov, D. A. Livshits, V. M. Ustinov, N. N. Ledentsov, D. Bimberg, and Z. I. Alferov, J. Cryst. Growth **251**, 729 (2003).
[21]J. Li, K. Worms, R. Maestle, D. Hillerkuss, W. Freude, and J. Leuthold, Opt. Express **19**, 11654 (2011).
[22]P. Borri, W. Langbein, J. M. Hvam, F. Heinrichsdorff, M.-H. Mao, and D. Bimberg, IEEE J. Sel. Top. Quantum Electron. **6**, 544 (2000).